Research Article

Rapid Communications in Mass Spectrometry

Received: 3 December 2010 Revised: 6 May 2011 Accepted: 15 May 2011 Published online in Wiley Online Library

Rapid Commun. Mass Spectrom. **2011**, *25*, 2153–2162
(wileyonlinelibrary.com) DOI: 10.1002/rcm.5097

Identification of phase I and phase II metabolites of benfluron and dimefluron in rat urine using high-performance liquid chromatography/tandem mass spectrometry

Robert Jirásko[1], Michal Holčapek[1]* and Milan Nobilis[2,3]

[1]Department of Analytical Chemistry, Faculty of Chemical Technology, University of Pardubice, Studentská 573, 53210 Pardubice, Czech Republic

[2]Department of Pharmaceutical Chemistry and Drug Control, Faculty of Pharmacy, Charles University, Heyrovského 1203, 500 05 Hradec Králové, Czech Republic

[3]Institute of Experimental Biopharmaceutics, Joint Research Centre of Academy of Sciences of the Czech Republic and PRO.MED.CS Praha a.s., Heyrovského 1207, 500 03 Hradec Králové, Czech Republic

Biotransformation products of two potential antineoplastic agents, benfluron and dimefluron, are characterized using our integrated approach based on the combination of high-performance liquid chromatography (HPLC) separation of phase I and phase II metabolites followed by photodiode-array UV detection and electrospray ionization tandem mass spectrometry (MS/MS). High mass accuracy measurement allows confirmation of an elemental composition and metabolic reactions according to exact mass defects. The combination of different HPLC/MS/MS scans, such as reconstructed ion current chromatograms, constant neutral loss chromatograms or exact mass filtration, helps the unambiguous detection of low abundance metabolites. The arene oxidation, N-oxidation, N-demethylation, O-demethylation, carbonyl reduction, glucuronidation and sulfation are typical mechanisms of the metabolite formation. The interpretation of their tandem mass spectra enables the distinction of demethylation position (N- vs. O-) as well as to differentiate N-oxidation from arene oxidation for both phase I and phase II metabolites. Two metabolic pathways are rather unusual for rat samples, i.e., glucosylation and double glucuronidation. The formation of metabolites that lead to a significant change in the chromophoric system of studied compounds, such as the reduction of carbonyl group in 7*H*-benzo[c]fluorene-7-one chromophore, is reflected in their UV spectra, which provides valuable complementary information to MS/MS data.

Antineoplastic agents are used as drugs in cancer chemotherapy. They involve a high number of compounds differing in chemical structures, mechanisms of anti-cancer action, suitability and sensibility for the treatment of various types of neoplasia or their metastases and in the disposition of these compounds in the treated organism.[1] The formation of drug metabolites is closely associated with chemical structures of studied compounds. Oxidation processes, such as hydroxylation or epoxidation, are common for aromatic systems; the presence of a carboxyl group can result in decarboxylation, the methyl substituent on the heteroatom can be lost by demethylation, etc.[2] The formation of phase I and phase II metabolites is closely related to enzymes that are present in studied organisms. In general, different metabolites can be found for various species or even for different tissues of particular organisms.[3]

* *Correspondence to:* M. Holčapek, Department of Analytical Chemistry, Faculty of Chemical Technology, University of Pardubice, Studentská 573, 53210 Pardubice, Czech Republic.
E-mail: Michal.Holcapek@upce.cz

The characterization of new drugs, identification and structure elucidation of their phase I and II metabolites is an important step for the drug research and development. High-performance liquid chromatography/tandem mass spectrometry (HPLC/MS/MS) is usually a method of choice for the metabolic studies due to high sensitivity and structural information even for trace metabolites in highly complex matrices.[2] Several strategies, such as the use of selected tandem mass spectrometric scans, on-line hydrogen/deuterium (H/D) exchange HPLC/MS/MS, accurate mass measurements, radio-labeling of parent drugs, chemical derivatization to determine the metabolite position or to improve ionization efficiency, softwares dedicated to the metabolite prediction or detection can be applied for this purpose.[2,4–6] The optimization of HPLC conditions is necessary to achieve high efficiency, sensitivity and speed.[7–10] Enantiomers of chiral drugs and their phase I and II metabolites can be separated on chiral columns.[11] Although the parent drug may not exhibit chirality, the chiral carbon atom can be formed by metabolic reactions, e.g., reduction of a carbonyl group by an enzyme from the aldo-keto reductase family in the case of flubendazol,[12] pentoxifylline[13] or benzo[*c*]fluorene drugs.[14]

Concerning studied compounds, benfluron (5-(2-dimethylaminoethoxy)-7*H*-benzo[*c*]fluoren-7-one hydrochloride) belongs to the first generation of basic benzo[*c*]fluorene

antineoplastic agents that provide an interesting spectrum of pharmacodynamic properties in experiments *in vitro* and *in vivo*.[15] Dimefluron (3,9-dimethoxy-5-(2-dimethylaminoethoxy)-7*H*-benzo[*c*]fluoren-7-one hydrochloride) is a typical representative of the second generation of basic benzo[*c*]fluorenes synthesized as a structural modification of benfluron leading to the improvement of pharmacokinetic, distribution and xenobiochemical properties in comparison to benfluron. The biotransformation of benfluron and dimefluron in experimental animals has been studied by various methods using the comparison of chromatographic and spectral properties of the parent drug and several synthesized metabolites, but no information about the formation of phase II metabolites (except one glucuronide) has been reported. Most previous works describe only UV spectra of phase I metabolites and their comparison with synthetic standards.[14–17] Two articles only contain some MS data. First, HPLC/MS with fast atom bombardment has been tested for the identification of benfluron metabolites,[15] but this technique is not convenient for the identification of drug metabolites in complex biomatrices at low concentrations. The second work provides information about some basic phase I metabolites of dimefluron using electrospray ionization (ESI) and atmospheric pressure chemical ionization, but no phase II metabolites of dimefluron have been examined in this study.[16]

In our study, phase II metabolites of benfluron and dimefluron are studied in rat biotransformation samples using our integrated approach based on a combination of different techniques. The power of this approach is demonstrated by the identification of 30 different metabolites for both studied drugs.

EXPERIMENTAL

Materials

Acetonitrile (HPLC gradient grade), formic acid and sodium formate were purchased from Sigma-Aldrich (St. Louis, MO, USA). De-ionized water was prepared with a Demiwa 5-roi purification system (Watek, Ledeč nad Sázavou, Czech Republic).

Benfluron and its phase I metabolites

Benfluron, 5-(2-dimethylaminoethoxy)-7*H*-benzo[*c*]fluoren-7-one ($C_{21}H_{19}NO_2$, molecular weight (MW) = 317.1416 Da, Fig. 1) was synthesized in the former Research Institute for Pharmacy and Biochemistry (Prague, Czech Republic). Reduced benfluron, 5-(2-dimethylaminoethoxy)-7*H*-benzo[*c*]fluoren-7-ol (base) ($C_{21}H_{21}NO_2$, MW = 319.1572 Da) and other phase I metabolites were synthesized in our laboratories, as reported earlier.[15] Standards were transformed into the corresponding salts and used in the form of hydrochlorides with the exception of reduced benfluron.

Dimefluron and its phase I metabolites

Dimefluron, 3,9-dimethoxy-5-(2-dimethylaminoethoxy)-7*H*-benzo[*c*]fluoren-7-one ($C_{23}H_{23}NO_4$, MW = 377.1627 Da, Fig. 1); 9-*O*-demethyldimefluron, 9-hydroxy-3-methoxy-5-(2-dimethylaminoethoxy)-7*H*-benzo[*c*]fluoren-7-one ($C_{22}H_{21}NO_4$, MW = 363.1471 Da); 3-*O*-demethyldimefluron, 3-hydroxy-9-methoxy-5-(2-dimethylaminoethoxy)-7*H*-benzo[*c*]fluoren-7-one hydrochloride ($C_{22}H_{21}NO_4$, MW = 363.1471 Da); C7-reduced dimefluron, 3,9-dimethoxy-5-(2-dimethylamino-ethoxy)-7*H*-benzo[*c*]fluoren-7-ol (base) ($C_{23}H_{25}NO_4$, MW = 379.1784 Da) were synthesized in our laboratories.[16] Standards were transformed into the corresponding salts and used in the form of hydrochlorides with the exception of reduced dimefluron.

Sample preparation of rat urine

Benfluron or dimefluron in parallel experiments was administered in a single oral dose of 250 mg.kg^{-1} of body weight to male rats (*Rattus norvegicus* var. *alba*, Wistar type, weight 290 g, Konárovice Breeding Station, Czech Republic) in the form of a saturated aqueous solution via a gastric probe. Experiments were approved by the Institutional Ethics Committee. Rats were placed individually into metabolic cages, where they had free access to water and food pellets before and during the experiment. Urine of individual rats was collected for 36 h after the administration of the corresponding benzo[*c*]fluorene derivative and stored at −70°C

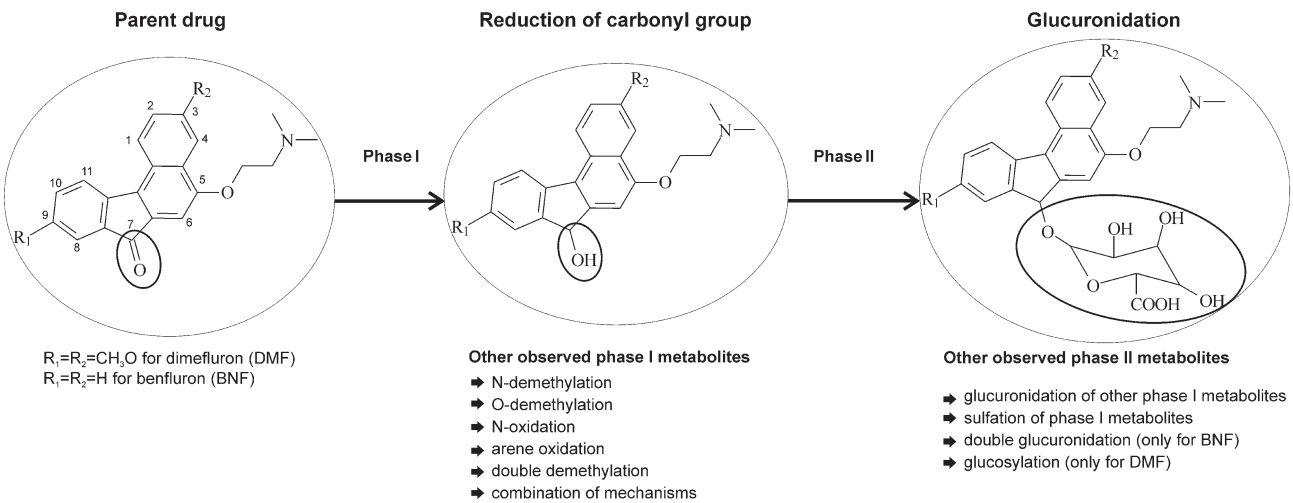

Figure 1. Structures of studied antineoplastic drugs together main observed phase I and phase II metabolic reactions.

Table 1. List of main peaks for dimefluron biotransformation sample detected by HPLC/MS with their retention times, relative retention shifts, *m/z* values of their $[M+H]^+$ and $[M–H]^-$ ions, mass accuracies, elemental composition and the description of metabolite formation

Retention time [min]	Relative retention shift	$[M+H]^+$ Experimental *m/z*	$[M+H]^+$ Mass accuracy [ppm]	$[M-H]^-$ Experimental *m/z*	$[M-H]^-$ Mass accuracy [ppm]	Compound elemental composition	Description of metabolite formation: Phase I	Description of metabolite formation: Phase II
9.8	0.45	542.2026	0.9	540.1865	−1.9	$C_{28}H_{31}NO_{10}$	carbonyl reduction, demethylation	glucuronide
10.2	0.47	526.1706	−0.4	524.1572	1.9	$C_{27}H_{27}NO_{10}$	2*demethylation	glucuronide
10.4	0.48	540.1861	−0.6	538.1716	−0.6	$C_{28}H_{29}NO_{10}$	demethylation	glucuronide
10.4	0.48	558.1941	−5.2	556.1824	0.0	$C_{28}H_{31}NO_{11}$	carbonyl reduction, demethylation, oxidation	glucuronide
10.5	0.48	528.1851	−2.5	526.1704	−2.9	$C_{27}H_{29}NO_{10}$	carbonyl reduction, 2*demethylation	glucuronide
10.6	0.49	542.2013	−1.5	540.1871	−0.7	$C_{28}H_{31}NO_{10}$	carbonyl reduction, demethylation	glucuronide
11.6	0.53	396.1812	1.8	n.d.[a]	–	$C_{23}H_{25}NO_5$	oxidation, carbonyl reduction	–
11.7	0.54	352.1541	−0.6	n.d.[a]	–	$C_{21}H_{21}NO_4$	2*demethylation, carbonyl reduction	–
12.0	0.55	366.1685	−4.1	364.1546	−2.2	$C_{22}H_{23}NO_4$	demethylation, carbonyl reduction	–
12.1	0.56	352.1546	0.9	350.1394	−1.1	$C_{21}H_{21}NO_4$	2*demethylation, carbonyl reduction	–
12.2	0.56	542.2015	−1.1	540.1876	0.2	$C_{28}H_{31}NO_{10}$	carbonyl reduction, demethylation	glucuronide
12.9	0.59	432.1143	7.2	430.0976	2.3	$C_{21}H_{21}NO_7S$	carbonyl reduction, 2*demethylation	sulfate
13.0	0.60	526.1710	0.4	524.1560	−0.4	$C_{27}H_{27}NO_{10}$	2*demethylation	glucuronide
13.1	0.60	540.1851	−2.4	538.1720	0.2	$C_{28}H_{29}NO_{10}$	demethylation	glucuronide
13.3	0.61	446.1269	0.2	444.1125	0.7	$C_{22}H_{23}NO_7S$	carbonyl reduction, demethylation	sulfate
13.4	0.62	394.1650	0.3	n.d.[a]	–	$C_{23}H_{23}NO_5$	oxidation	–
13.5	0.62	350.1370	−4.9	348.1228	−3.7	$C_{21}H_{19}NO_4$	2*demethylation	–
13.6	0.63	542.2362	−4.2	540.2221	−3.3	$C_{29}H_{35}NO_9$	carbonyl reduction	glucoside
13.7	0.63	394.1650	0.3	392.1495	−2.0	$C_{23}H_{23}NO_5$	oxidation	–
13.8	0.64	364.1534	−2.5	362.1399	0.3	$C_{22}H_{21}NO_4$	9-O-demethylation	–
14.3	0.66	542.2013	−1.5	540.1864	−2.0	$C_{28}H_{31}NO_{10}$	carbonyl reduction, demethylation	glucuronide
14.6	0.67	556.2174	−0.5	554.2026	−1.1	$C_{29}H_{33}NO_{10}$	carbonyl reduction	glucuronide
14.8	0.68	430.0931	−5.6	428.0803	−1.4	$C_{21}H_{19}NO_7S$	2*demethylation	sulfate
15.3	0.71	444.1137	5.6	442.0956	−2.3	$C_{22}H_{21}NO_7S$	demethylation	sulfate
15.3	0.71	350.1399	3.4	348.1226	−4.3	$C_{21}H_{19}NO_4$	2*demethylation	–
15.7	0.72	542.2036	2.8	540.1860	−2.8	$C_{28}H_{31}NO_{10}$	carbonyl reduction, demethylation	glucuronide
16.0	0.74	364.1548	1.4	362.1399	0.3	$C_{22}H_{21}NO_4$	3-O-demethylation	–
16.2	0.75	556.2181	0.7	554.2021	−2.0	$C_{29}H_{33}NO_{10}$	carbonyl reduction	glucuronide
16.5	0.76	380.1868	3.2	n.d.[a]	–	$C_{23}H_{25}NO_4$	carbonyl reduction	–
18.6	0.86	396.1814	2.3	394.1654	−1.5	$C_{23}H_{25}NO_5$	oxidation, carbonyl reduction	–
21.1	0.97	364.1534	−2.5	n.d.[a]	–	$C_{22}H_{21}NO_4$	N-demethylation	–
21.7	**1.00**	**378.1706**	**1.6**	**n.d.**[a]	–	**$C_{23}H_{23}NO_4$**	**dimefluron (parent drug)**	–
23.4	1.08	394.1657	2.0	n.d.[a]	–	$C_{23}H_{23}NO_5$	N-oxidation	–

[a]n.d. – not detected.

Table 2. List of main peaks for benfluron biotransformation sample detected by HPLC/MS with their retention times, relative retention shifts, *m/z* values of their $[M+H]^+$and $[M–H]^-$ ions, mass accuracies, elemental composition and the description of metabolite formation

Retention time [min]	Relative retention shift	$[M+H]^+$ Experimental *m/z*	$[M+H]^+$ Mass accuracy [ppm]	$[M–H]^-$ Experimental *m/z*	$[M–H]^-$ Mass accuracy [ppm]	Compound elemental composition	Description of metabolite formation: Phase I	Description of metabolite formation: Phase II
6.5	0.27	690.1995	−4.9	688.1894	1.6	$C_{32}H_{35}NO_{16}$	carbonyl reduction, demethylation, 2*oxidation	2*glucuronide
7.3	0.31	498.1732	−5.4	496.1621	1.6	$C_{26}H_{27}NO_9$	carbonyl reduction, demethylation, oxidation	glucuronide
7.4	0.31	512.1900	−2.9	510.1753	−3.3	$C_{27}H_{29}NO_9$	carbonyl reduction, oxidation	glucuronide
8.0	0.34	512.1915	0.0	510.1774	0.8	$C_{27}H_{29}NO_9$	carbonyl reduction, oxidation	glucuronide
8.5	0.36	674.2064	−2.2	672.1947	1.9	$C_{32}H_{35}NO_{15}$	carbonyl reduction, demethylation, oxidation	2*glucuronide
8.5	0.36	496.1583	−3.8	494.1458	0.2	$C_{26}H_{25}NO_9$	demethylation, oxidation	glucuronide
9.0	0.38	510.1749	−2.0	508.1627	2.8	$C_{27}H_{27}NO_9$	oxidation	glucuronide
9.2	0.39	688.2213	−3.3	686.2113	3.4	$C_{33}H_{37}NO_{15}$	carbonyl reduction, oxidation	2*glucuronide
9.4	0.40	528.1861	−0.6	526.1717	−0.4	$C_{27}H_{29}NO_{10}$	carbonyl reduction, 2*oxidation	glucuronide
9.9	0.42	528.1858	−1.1	526.1715	−0.8	$C_{27}H_{29}NO_{10}$	carbonyl reduction, 2*oxidation	glucuronide
10.7	0.45	526.1675	−6.3	524.1555	−1.3	$C_{27}H_{27}NO_{10}$	2*oxidation	glucuronide
12.7	0.54	322.1437	−0.3	320.1283	−2.8	$C_{20}H_{19}NO_3$	carbonyl reduction, oxidation, demethylation	–
13.5	0.57	336.1592	−0.6	334.1439	−3.0	$C_{21}H_{21}NO_3$	carbonyl reduction, oxidation	–
14.1	0.59	512.1880	−6.8	510.1767	−0.6	$C_{27}H_{29}NO_9$	carbonyl reduction, oxidation	glucuronide
15.0	0.63	402.0987	−4.7	400.0866	1.5	$C_{20}H_{19}NO_6S$	carbonyl reduction, demethylation, oxidation	sulfate
15.4	0.65	512.1903	−2.3	510.1767	−0.6	$C_{27}H_{29}NO_9$	carbonyl reduction, oxidation	glucuronide
15.5	0.65	352.1548	1.4	350.1405	2.0	$C_{21}H_{21}NO_4$	carbonyl reduction, 2*oxidation	–
15.8	0.67	416.1157	−1.2	414.1027	2.4	$C_{21}H_{21}NO_6S$	carbonyl reduction, oxidation	sulfate
16.5	0.70	320.1282	0.3	318.1146	3.1	$C_{20}H_{17}NO_3$	demethylation, oxidation	–
17.1	0.72	334.1441	0.9	332.1297	1.5	$C_{21}H_{19}NO_3$	oxidation	–
17.8	0.75	496.1928	−7.7	494.1823	0.6	$C_{27}H_{29}NO_8$	carbonyl reduction	glucuronide
17.9	0.76	400.0841	−2.0	398.0703	−0.3	$C_{20}H_{17}NO_6S$	demethylation, oxidation	sulfate
18.4	0.78	414.0995	−2.7	412.0858	−0.5	$C_{21}H_{19}NO_6S$	oxidation	sulfate
19.1	0.81	350.1374	−3.7	348.1243	0.6	$C_{21}H_{19}NO_4$	2*oxidation	–
19.6	0.83	496.1938	−5.6	494.1845	5.1	$C_{27}H_{29}NO_8$	carbonyl reduction	glucuronide
19.9	0.84	320.1633	−3.7	n.d.[a]	–	$C_{21}H_{21}NO_2$	carbonyl reduction	–
21.8	0.92	512.1888	−5.3	510.1772	0.4	$C_{27}H_{29}NO_9$	carbonyl reduction, oxidation	glucuronide
23.7	**1.00**	**318.1476**	**−4.1**	**n.d.**[a]	–	**$C_{21}H_{19}NO_2$**	**benfluron (parent drug)**	–
25.9	1.09	334.1416	−6.6	332.1298	1.8	$C_{21}H_{19}NO_3$	N–oxidation	–

[a]n.d. – not detected.

Rapid Communications in Mass Spectrometry

Rapid Communications in Mass Spectrometry

until the HPLC/MS/MS analysis. Rat urine was filtered and subsequently diluted five times with a mixture of acetonitrile/water (1:1, v/v).

HPLC/MS/MS

HPLC/MS/MS chromatograms of samples were recorded in both positive and negative polarity modes using electrospray ionization (ESI) and a hybrid QqTOF mass analyzer (micrOTOF-Q, Bruker Daltonics, Germany). HPLC was performed on an Agilent 1200 series liquid chromatograph (Agilent Technology, Waldbronn, Germany) using a Luna C18 column (250 × 2 mm, 5 µm; Phenomenex, Torrance, CA, USA), at a flow rate of 0.4 mL/min and an injection volume of 1 µL. The mobile phase consisted of water (A) and acetonitrile (B), both with the addition of 0.1% formic acid. The linear gradient for benfluron was as follows: 0 min – 14% B, 22 min – 30% B, 32 min – 90% B; and finally washing and reconditioning of the column. The linear gradient for dimefluron was as follows: 0 min – 10% B, 8 min – 26% B, 12 min – 26% B, 22 min – 35% B, 32 min – 90% B; and finally washing and reconditioning of the column. The QqTOF mass spectrometer was used with the following settings of tuning parameters: capillary voltage ±4.5 kV, drying temperature 210°C, the flow rate and pressure of nitrogen were 9 L/min and 1.4 bar, respectively. The external calibration was performed with sodium formate clusters before individual measurements. ESI mass spectra were recorded in the range of *m/z* 50–1000 both in positive and negative ion modes. The isolation width Δ*m/z* 6 and the collision energy in the range of 20 to 22 eV using argon as the collision gas were used for MS/MS experiments. An ion trap analyzer (Esquire 3000, Bruker Daltonics, Germany) was used for multistage MS measurements. The software package Metabolite tool containing two algorithms Metabolite predict and Metabolite detect (Bruker Daltonics, Bremen, Germany) was used for the metabolite detection.

RESULTS AND DISCUSSION

The difference between benfluron (BNF) and dimefluron (DMF) consists in the substitution of C3 and C9 on the arene ring (see Fig. 1). Two methoxy groups are present for DMF, whereas BNF has no substitution in these positions. Possible metabolites can be predicted based on the structure of parent drugs using the appropriate software and the knowledge of fragmentation behavior associated with metabolic reactions.[2] The presence of four methyl substituents for DMF leads to the logical prediction that the demethylation is the basic phase I metabolic reaction in comparison to BNF, where the hydroxylation prevails (see Tables 1 and 2). The main metabolic pathways for both studied compounds are shown in Fig. 1. All observed metabolites are summarized in Tables 1 and 2. ESI full scan and tandem mass spectra

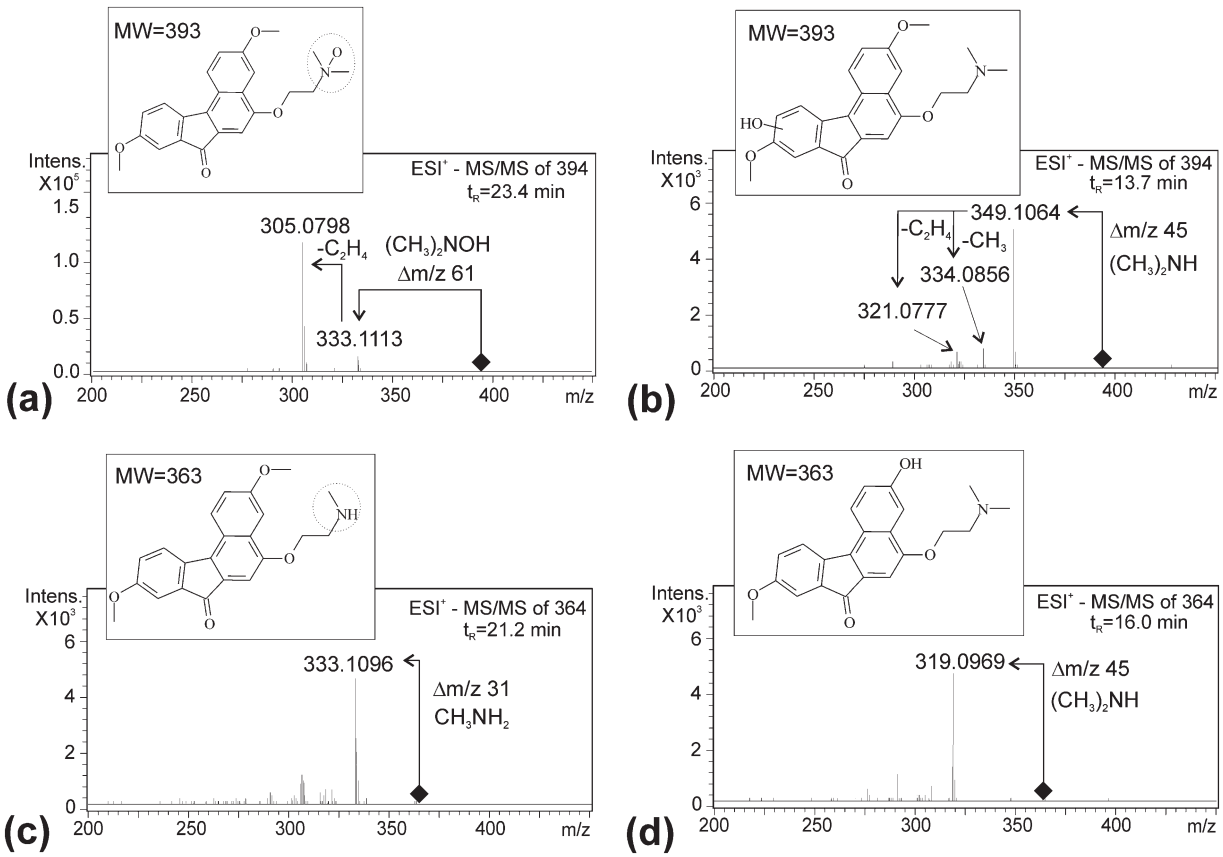

Figure 2. Positive ion ESI-MS/MS spectra of protonated molecules together with proposed structures of (a) dimefluron *N*-oxide, (b) hydroxylated dimefluron, (c) N-demethylated dimefluron, and (d) 3-O-demethylated dimefluron.

in both polarity modes were measured for all studied samples. The positive ion ESI mode provides better sensitivity and higher information content for the metabolite identification.

Phase I metabolites

The products of demethylation, hydroxylation, N-oxidation, carbonyl reduction and their combinations are detected as phase I metabolites. The position of hydroxylation or demethylation can be determined in different ways. The most reliable is the comparison with identical standards using matching of retention times and fragmentation patterns. Three phase I metabolites for DMF (3-*O*-demethyldimefluron, 9-*O*-demethyldimefluron, reduced DMF) and one for BNF (reduced BNF) have been synthesized. Other metabolites are identified based on high mass accuracy measurements (<3 ppm), information from tandem mass spectra, UV spectra and known typical relative retention shifts.[2] N- or O-demethylation as well as hydroxylation or N-oxidation are distinguished according to characteristic neutral losses (NLs). Figure 2 illustrates four tandem mass spectra of phase I DMF metabolites. For hydroxylated products or O-demethylation, the characteristic NL of the dimethylamine group $\Delta m/z$ 45 from the side chain is the same as for the parent drug. However, metabolites with structural changes on the dimethylamino group (N-demethylation or N-oxidation) show different NLs.[16] The NL of $\Delta m/z$ 61 $(CH_3)_2NOH$ is observed for N-oxidation and $\Delta m/z$ 31 CH_3NH_2 for N-demethylation. Moreover, the higher retention is typical for N-oxides and N-demethylated metabolites. NLs of $\Delta m/z$ 16 or 17, typical for N-oxides,[18] are not present in this case.

The formation of C9 hydroxylated metabolites is the most probable phase I metabolic process for BNF. In general, the position of hydroxylation cannot be distinguished based on mass spectra, but UV spectra can yield valuable information in this respect.[15] Although the hydroxylation on C9 was confirmed for most observed hydroxylated metabolites of BNF, the UV signal for some trace metabolites is too low for unambiguous conclusion on the hydroxylation position. Both drugs have an aromatic system containing nine double bonds in conjugation, which yields characteristic UV spectra. The metabolic reduction of a carbonyl group to a hydroxyl group causes the interruption of this conjugated system with a well-pronounced effect on the UV spectra of both drugs (Fig. 3), which enables separation of all the metabolites into two distinct groups depending on the reduced or non-reduced carbonyl group in the C7 position (see Fig. 1).

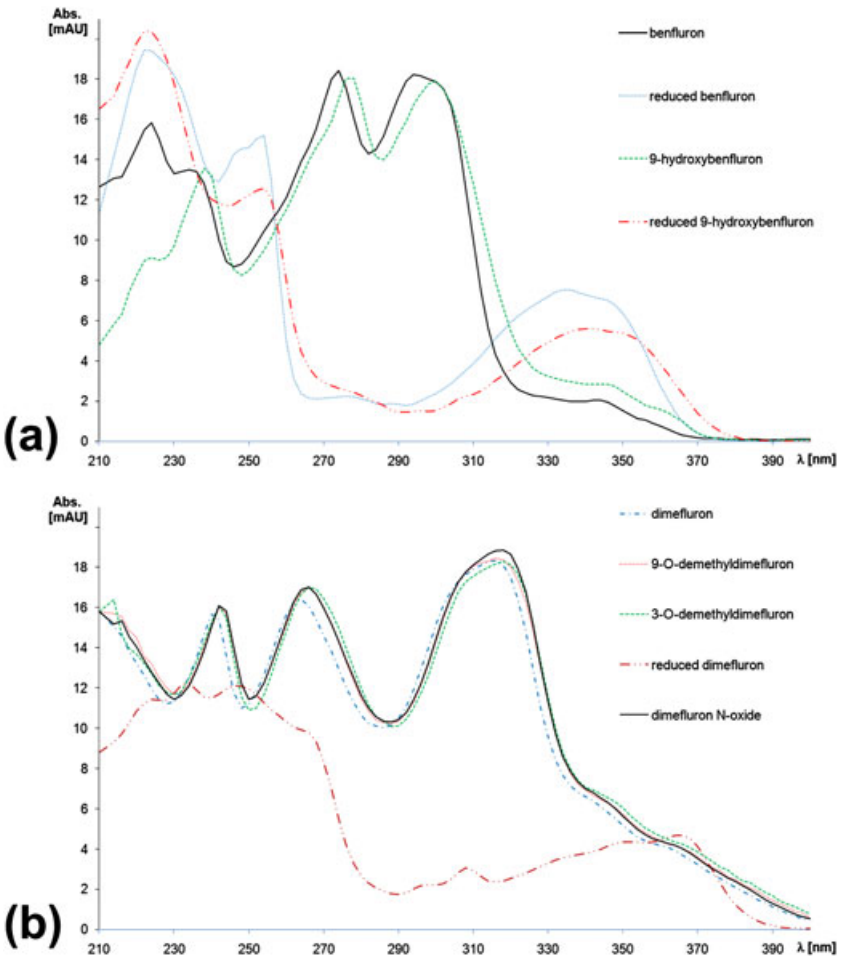

Figure 3. Comparison of UV spectra for main phase I metabolites of (a) benfluron and (b) dimefluron.

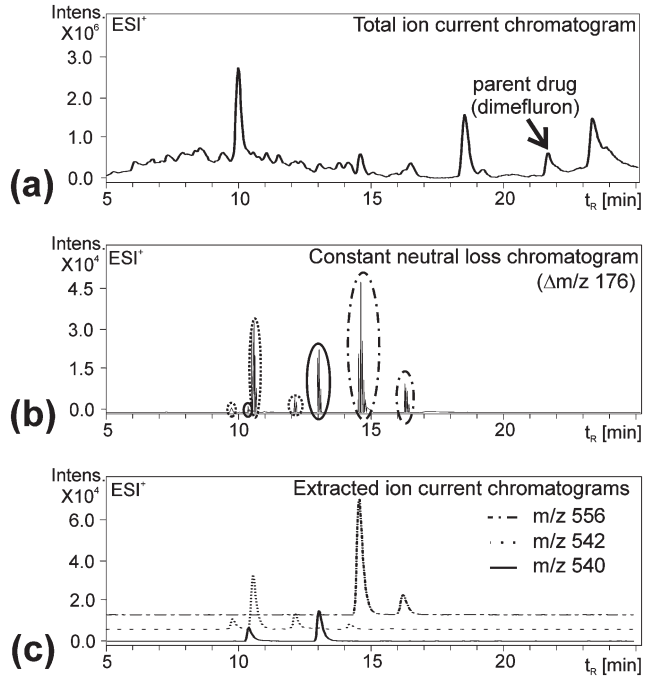

Figure 4. Scan modes in HPLC/MS/MS used for the metabolite detection of dimefluron biotransformation: (a) total ion current chromatogram, (b) constant neutral loss chromatogram of Δ*m/z* 176, and (c) extracted ion current chromatograms of *m/z* 556, 542 and 540.

Phase II metabolites

Several scan types are used for the HPLC/MS/MS identification of metabolic pathways of studied drugs, as illustrated in Fig. 4 for DMF. The presence of numerous coeluting peaks that correspond to various compounds of both exogenous and endogenous origin in the TIC chromatogram (Fig. 4(a)) significantly complicates the data interpretation. The first step is the known fragmentation behavior of phase II conjugates, i.e., characteristic NLs for glucuronides are Δ*m/z* 194 ($C_6H_{10}O_7$) and 176 ($C_6H_8O_6$), for sulfates Δ*m/z* 98 (H_2SO_4) and 80 (SO_3).[2] The constant NL Δ*m/z* 176 chromatogram for rat urine with DMF metabolites (Fig. 4(b)) clearly shows all peaks providing this NL and therefore preliminary assigned as glucuronides. The next step is the use of extracted ion current chromatograms (Fig. 4(c)) for *m/z* values observed for peaks detected in the constant NL scan with the defined tolerance of mass error. The resolving power and mass accuracy of the QqTOF analyzer used for this study enable an extraction of individual chromatograms in a narrow interval (±5 mDa) that eliminates possible interferences from similar masses. Clear correlations are observed among these scans, which can be verified by perfect match of overlaid chromatograms (not shown). Extracted ion current (EIC) chromatograms visualize peak profiles for individual metabolites, which is subsequently used for the exact determination of time intervals for the measurement of the mass spectrum and background subtraction. This procedure improves the quality of recorded mass spectra, which is quite an important issue in the case of trace metabolites in complex biological matrices. Ions with intensity below the defined fragmentation threshold are not included in the constant NL chromatogram and therefore less metabolites are recorded here in comparison with EIC chromatograms. MS/MS spectra of these low abundance ions can be recorded with the repetitive experiment with increased dosing, decreased automatic fragmentation threshold or by manual setting of the required *m/z* value. Moreover, the comparison with chromatograms of a placebo experiment confirms the origin of detected compounds.

Our approach to the identification of combined phase I and II metabolic reactions is illustrated on three model examples in Table 3. The NL loss Δ*m/z* 176 is proof of glucuronide conjugation. Then, this NL ($C_6H_8O_6$) is subtracted from the metabolite molecule (e.g., from the metabolite $C_{28}H_{29}NO_{10}$ with MW = 539), which leads to the difference I (in this example $C_{22}H_{21}NO_4$). Finally, the elemental composition of the initial drug is subtracted, which results in the difference II. The negative difference Δ*m/z* = −14 (CH_2) corresponds to demethylation. The description of all metabolic pathways is clarified in a similar way.

In total, 16 glucuronides are identified for BNF and 13 for DMF (see Tables 1 and 2). Three double glucuronides are observed for BNF (see Table 2), which is not often reported in the literature. The typical feature of double glucuronidation is a higher mass defect, higher MWs and characteristic tandem mass spectra, where NLs of both glucuronides are observed (Fig. 5). The relatively high abundance ion at *m/z* 247 is formed by the NL of Δ*m/z* 57 CH_3NCHCH_3 from *m/z* 304, which confirms N-demethylation.

Concerning sulfate metabolites, their number is lower compared to glucuronides (see Tables 1 and 2). Four sulfates for each studied compound are observed in both positive and negative ion full scan mass spectra. The signal for sulfates in the positive ion mode is observed only in the case where the suitable protonation site is present in the molecules, such as the tertiary *N,N*-dimethylamino group. The C9 hydroxylation for BNF or the demethylation in case of DMF precede the sulfate conjugation in agreement with above-mentioned phase I metabolism. The change in relative

Table 3. Description of metabolic pathways for three types of glucuronides with MW = 539, 541 and 555 Da

	Elemental composition				
MW	Metabolite	Neutral loss Δ*m/z*176 (phase II reaction)	Difference I	Initial drug	Difference II (phase I reaction)
539	$C_{28}H_{29}NO_{10}$	$-C_6H_8O_6$	$C_{22}H_{21}NO_4$	$-C_{23}H_{23}NO_4$	$-CH_2$
541	$C_{28}H_{31}NO_{10}$		$C_{22}H_{23}NO_4$		C ($-CH_2 + H_2$)
555	$C_{29}H_{33}NO_{10}$		$C_{23}H_{25}NO_4$		$+H_2$

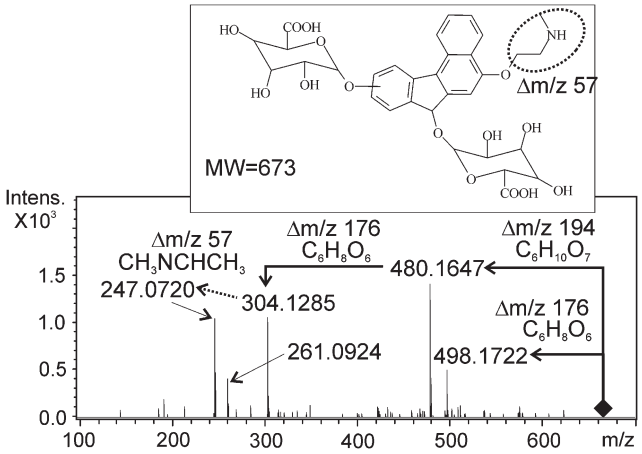

Figure 5. Positive ion ESI-MS/MS spectrum of protonated molecule for benfluron diglucuronide (MW = 673) together with its proposed structure.

abundances of M + 2 isotopic peaks is in accordance with the presence of one sulfur atom in sulfates (see Fig. 6(a)).

The fragmentation pathway of the protonated molecule of sulfate with MW = 415 is shown in Fig. 6(b). Characteristic NLs Δ*m/z* 98 (H_2SO_4) and Δ*m/z* 80 (SO_3) correspond with common fragmentation behavior of sulfates.[18] These fragment ions observed already in the full scan mass spectra are related to the low stability of the sulfate functional group. Furthermore, NLs of Δ*m/z* 125 (Δ*m/z* 45 + Δ*m/z* 80) and Δ*m/z* 143 (Δ*m/z* 45 + Δ*m/z* 98) confirm the presence of a dimethylamino group similarly as for phase I metabolites. The fragmentation of the deprotonated molecule (Fig. 6(c)) yields the stable radical ion at *m/z* 262 $[M\text{-}H\text{-}SO_3\text{-}(CH_3)_2NCH_2CH_2]^{-\cdot}$ and only a low signal is recorded for the common NL of SO_3.

In general, NLs Δ*m/z* 45 or 71 confirm the presence of N $(CH_3)_2$ and exclude demethylation on the nitrogen atom (Figs. 6(b) and 6(d)). On the other hand, the intensive NLs including Δ*m/z* 57 or 31 as well as their combination with NLs of Δ*m/z* 80 or 98 are observed in the case of N-demethylated sulfate metabolites (Figs. 6(e) and 6(f)).

The same approach can be used for the verification of N-demethylation in the case of glucuronides. NLs of Δ*m/z* 221 (Δ*m/z* 176 + Δ*m/z* 45) and Δ*m/z* 239 (Δ*m/z* 194 + Δ*m/z* 45) are observed for metabolites with an unchanged dimethylamine group, e.g., metabolites corresponding to demethylation and subsequent glucuronidation of DMF (MW = 539). Two metabolites of this type are found for DMF and none for BNF (Tables 1 and 2), which proves that the demethylation is not situated on the nitrogen atom but on the methoxy group. 9-*O*-Demethylated DMF glucuronide should elute first considering the analogy with phase I metabolites (3-*O*-demethyldimefluron and 9-*O*-demethyldimefluron).

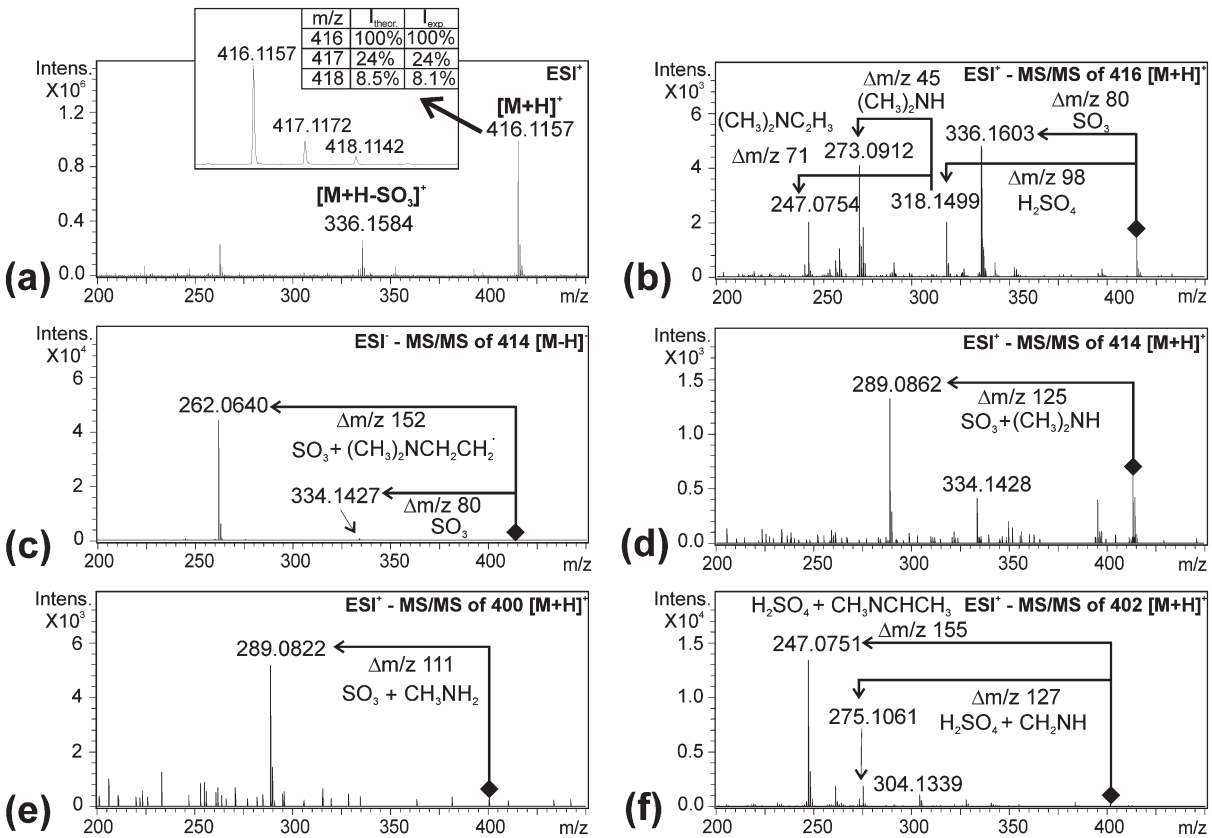

Figure 6. ESI mass spectra of benfluron sulfates: (a) positive ion full scan mass spectrum of peak at 15.8 min with the comparison of experimental and theoretical isotopic abundances of *m/z* 416; (b) negative ion MS/MS spectrum of *m/z* 416 for sulfate eluted in 15.8 min; (c) positive ion MS/MS spectrum of *m/z* 414 for sulfate eluted in 15.8 min; (d) positive ion MS/MS spectrum of *m/z* 414 for sulfate eluted in 18.4 min; (e) positive ion MS/MS spectrum of *m/z* 400 for sulfate eluted in 17.9 min; and (f) positive ion MS/MS spectrum of *m/z* 402 for sulfate eluted in 15 min.

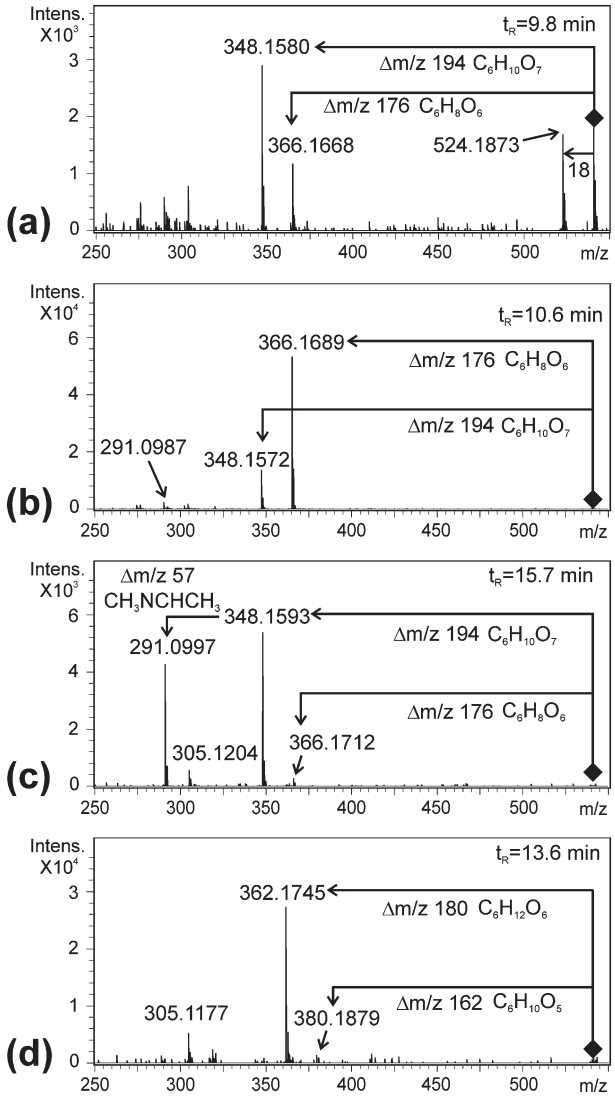

Figure 7. Differentiation of dimefluron glucuronides and glucoside based on MS/MS spectra for chromatographic peaks with the following retention times (t_R): (a) glucuronide at $t_R = 9.8$ min, (b) glucuronide at $t_R = 10.6$ min, (c) glucuronide at $t_R = 15.7$ min, and (d) glucoside at $t_R = 13.6$ min.

Figure 7 represents tandem mass spectra of four different protonated phase II metabolites. Three of them have identical elemental composition ($C_{28}H_{31}NO_{10}$) and correspond to the metabolites formed by carbonyl reduction, demethylation and subsequent glucuronidation. The latter metabolite has the summary formula $C_{29}H_{35}NO_9$ formed by carbonyl reduction and glucosylation. Both metabolic pathways can be distinguished using tandem mass spectra measurement. Typical NLs for glucosylation (Fig. 7(d)) are $\Delta m/z$ 180 and 162 instead of NLs of $\Delta m/z$ 176 and 194 typical for glucuronidation (see Figs. , 7(a)–7(c)).

Particular glucuronides with MW = 541 differ in positions of demethylation and glucuronidation. Fragment ions of expected NLs 176 and 194 are observed for all three compounds but with different intensity (see Fig. 7). Their identical standards or nuclear magnetic resonance spectra would be necessary for the determination of the exact position of glucuronidation. The significantly increased relative abundance of the ion at *m/z* 291 formed by NLs of CH_3NCHCH_3 ($\Delta m/z$ 57) from *m/z* 348 is observed for glucuronide eluted in 15.7 min (Fig. 7(c)) and confirms that the demethylation occurs at the nitrogen atom. The same fragmentation pattern is observed for the glucuronide eluted in 14.3 min. Their higher retention is also in agreement with N-demethylation.[2] Based on the fragmentation pattern, the glucuronidation is not placed on the secondary amino group but on the hydroxyl formed by the carbonyl reduction. The carbonyl reduction results in the formation of a chiral carbon atom for reduced DMF and BNF.[14] The coelution of both enantiomers is observed in the case of our separation in a non-chiral environment. The subsequent glucuronidation (glucuronic acid is an optically active compound) results in the formation of two diastereoisomers, which are separated on the C18 column, as evident from Tables 1 and 2 (e.g., two ions at *m/z* 542 for DMF – the difference between their retention times is 1.4 min; *m/z* 496 for BNF – difference is 1.8 min or *m/z* 556 for DMF – difference is 1.6 min). In general, two diastereoisomers of phase II metabolites are formed after the carbonyl reduction from particular enantiomers. A similar approach is used for the target separation of some enantiomers that are purposely exposed to the controlled reaction with other optically active compounds resulting in the formation of two diastereoisomers separated on a common C18 column.[11]

CONCLUSIONS

The identification of a wide range of phase I and II metabolites leads to a better understanding of biotransformation processes of studied antineoplastic agents and may provide perspectives for their potential pharmaceutical applications. In this study, 32 metabolites for dimefluron and 28 metabolites for benfluron were detected in the rat urine within 25 min. The identification of individual biotransformation products is performed using high mass accuracy measurements for both full scan and tandem mass spectra, extracted ion chromatograms for expected masses of metabolites together with the information about characteristic neutral losses (constant neutral loss chromatograms and fragmentation patterns). Results are supported by UV spectra of individual chromatographic peaks, the comparison of chromatograms of rat urine with the placebo experiment and correlation with previous literature data. Notable differences in biotransformation products between dimefluron and benfluron samples demonstrate that substituents on studied drugs markedly effect the formation of phase I and II metabolites. As for dimefluron, the demethylation is the main phase I metabolic reaction unlike benfluron, where the arylhydroxylation is preferred. Metabolites with structural changes on the dimethylamine group (N-demethylation or N-oxidation) provide different fragmentation patterns. Product ion mass spectra prove that conjugation phase II reactions take place only on present hydroxyls (phenol group formed newly via arylhydroxylation of the benzo[*c*]fluorene moiety, the secondary alcohol group created by C7-carbonyl reduction or the phenol group unmasked by O-demethylation of dimefluron). Phase II reactions on the amino group are not observed. Although no chiral separation is performed for the phase I reduced DMF (BNF) metabolites, the presence of two enantiomers is proved based on the identification of phase II diastereoisomers formed by glucuronidation.

Acknowledgements

This work was supported by Grant Nos. MSM0021627502 (MŠMT, Czech Republic) and MSM0021620822 (MŠMT, Czech Republic).

REFERENCES

[1] H. P. Rang, M. M. Dale, J. M. Ritter, R. J. Flower. *Rang and Dale's Pharmacology*. J & A Churchill, London, **2007**.
[2] M. Holčapek, L. Kolářová, M. Nobilis. *Anal. Bioanal. Chem.* **2008**, *391*, 59.
[3] B. Testa, S. D. Krämer. *The Biochemistry of Drug Metabolism: Conjugation, Consequences of Metabolism, Influencing Factors*. VHCA and Wiley-VCH, Zürich, **2010**.
[4] Q. D. Liu, A. C. E. C. Hop. *J. Pharm. Biomed. Anal.* **2005**, *37*, 1.
[5] F. R. Staack, G. Hopfgartner. *Anal. Bioanal. Chem.* **2007**, *388*, 1365.
[6] X. Liu, L. Jia. *Curr. Drug Metab.* **2007**, *8*, 815.
[7] D. Guillarme, J. Ruta, S. Rudaz, J. Veuthey. *Anal. Bioanal. Chem.* **2010**, *397*, 1069.
[8] Y. Hsieh. *J. Sep. Sci.* **2008**, *31*, 1481.
[9] L. Nováková, H. Vlčková. *Anal. Chim. Acta* **2009**, *656*, 8.
[10] K. Faure. *Electrophoresis* **2010**, *31*, 2499.
[11] S. Pérez, D. Barceló. *Trends Anal. Chem.* **2008**, *27*, 836.
[12] M. Nobilis, T. Jira, M. Lísa, M. Holčapek, B. Szotáková, J. Lamka, L. Skálová. *J. Chromatogr. A* **2007**, *1149*, 112.
[13] M. Nicklasson, S. Björkman, B. Roth, M. Jönsson, P. Höglund. *Chirality* **2002**, *14*, 643.
[14] R. Kučera, M. Nobilis, L. Skálová, B. Szotáková, P. Císař, T. Jira, J. Klimeš, V. Wsól. *J. Pharm. Biomed. Anal.* **2005**, *37*, 1049.
[15] M. Nobilis, P. Anzenbacher, J. Pastera, Z. Svoboda, K. Hrubý, J. Květina, K. Ubik, F. Trejtnar. *J. Chromatogr. B* **1996**, *681*, 143.
[16] P. Císař, M. Nobilis, Z. Vybíralová, M. Holčapek, L. Kolářová, M. Pour, J. Kuneš, J. Klimeš. *J. Pharm. Biomed. Anal.* **2005**, *37*, 1059.
[17] L. Skálová, M. Nobilis, B. Szotáková, E. Kondrová, M. Šavlík, V. Wsól, L. Pichard-Garcia, E. Maser. *Biochem. Pharmacol.* **2002**, *64*, 297.
[18] M. Holčapek, R. Jirásko, M. Lísa. *J. Chromatogr. A* **2010**, *1217*, 3908.

